



# Identification of a family of peptidoglycan transpeptidases reveals that Clostridioides difficile requires noncanonical cross-links for viability

Kevin W. Bollinger<sup>a</sup>, Ute Müh<sup>a</sup>, Karl L. Ocius<sup>b</sup>, Alexis J. Apostolos<sup>b,1</sup>, Marcos M. Pires<sup>b</sup>, Richard F. Helm<sup>c</sup>, David L. Popham<sup>d</sup>, David S. Weiss<sup>a,e,2</sup>, and Craig D. Ellermeier<sup>a,e,2</sup>

Affiliations are included on p. 10.

Edited by Joe Lutkenhaus, University of Kansas Medical Center, Kansas City, KS; received April 30, 2024; accepted July 12, 2024

Most bacteria are surrounded by a cell wall that contains peptidoglycan (PG), a large polymer composed of glycan strands held together by short peptide cross-links. There are two major types of cross-links, termed 4-3 and 3-3 based on the amino acids involved. 4-3 cross-links are created by penicillin-binding proteins, while 3-3 cross-links are created by L,D-transpeptidases (LDTs). In most bacteria, the predominant mode of cross-linking is 4-3, and these cross-links are essential for viability, while 3-3 cross-links comprise only a minor fraction and are not essential. However, in the opportunistic intestinal pathogen Clostridioides difficile, about 70% of the cross-links are 3-3. We show here that 3-3 cross-links and LDTs are essential for viability in C. difficile. We also show that C. difficile has five LDTs, three with a YkuD catalytic domain as in all previously known LDTs and two with a VanW catalytic domain, whose function was until now unknown. The five LDTs exhibit extensive functional redundancy. VanW domain proteins are found in many gram-positive bacteria but scarce in other lineages. We tested seven non-C. difficile VanW domain proteins and confirmed LDT activity in three cases. In summary, our findings uncover a previously unrecognized family of PG cross-linking enzymes, assign a catalytic function to VanW domains, and demonstrate that 3-3 cross-linking is essential for viability in *C. difficile*, the first time this has been shown in any bacterial species. The essentiality of LDTs in C. difficile makes them potential targets for antibiotics that kill *C. difficile* selectively.

peptidoglycan | C. difficile | transpeptidase

Clostridioides difficile is a gram-positive, spore-forming opportunistic pathogen that has become the leading cause of antibiotic-associated diarrhea in high-income countries. The CDC estimates that C. difficile infections kill over 12,000 people per year in the United States (1). C. difficile infections are often triggered by broad-spectrum antibiotics administered either prophylactically or to treat some other infection. These antibiotics have the unintended consequence of disrupting the intestinal microbiota that ordinarily keeps C. difficile in check (2, 3). The frontline treatment for *C. difficile* infections is vancomycin, which is usually effective but also kills desirable bacteria, so relapse rates exceed 20%, and for this cohort, the prognosis is poor (4–6). An antibiotic that kills *C. difficile* more selectively would presumably improve outcomes, but developing such a drug requires identifying targets uniquely important to C. difficile.

Many of our most useful antibiotics target biogenesis of the bacterial cell wall, which provides essential protection against lysis due to turgor pressure. The cell wall is composed of peptidoglycan (PG), a complex meshwork of glycan strands of alternating N-acetylglucosamine (NAG) and N-acetylmuramic acid (NAM) that are stitched together by short peptide cross-links (7, 8) (Fig. 1A). The predominant modes of cross-linking, termed 4-3 and 3-3, are named based on the position of the amino acids involved; 4-3 cross-links join a D-Alanine (D-Ala) in position four of one peptide to a meso-diaminopimelic acid (mDAP) in position three of another, while 3-3 cross-links join two mDAP residues (Fig. 1A). In Escherichia coli, about 90% of the cross-links are 4-3, and these are essential for viability, whereas only ~10% of the cross-links are 3-3 and these are not essential (9, 10). So far as is known, 3-3 cross-links are much less abundant than 4-3 cross-links in most other bacteria as well, although there are exceptions (11–18).

The two modes of cross-linking rely on completely different enzymes. All 4-3 cross-links are synthesized by D,D-transpeptidases, more commonly referred to as penicillin-binding proteins (PBPs) (19). PBPs catalyze a two-step transpeptidation reaction that starts with the nucleophilic attack of a catalytic serine on the amide bond linking D-Ala<sup>4</sup> to D-Ala<sup>5</sup> in a pentapeptide "donor" substrate. This reaction results in formation of a covalent acyl-enzyme intermediate and concomitant release of the terminal D-Ala. In the second step,

## **Significance**

Clostridioides difficile is an opportunistic pathogen that can cause significant intestinal health issues when gut microflora populations are disrupted. As the C. difficile peptidoglycan (PG) cell wall has an unusually high abundance of 3-3 cross-links. the enzymes synthesizing these structures, L,D-transpeptidases (LDTs), are potential drug targets. While three LDTs were previously known, deleting these genes caused minimal disruption to the PG structure. Here, we report the identification of a family of LDTs that are distinct from previously known LDTs. We show that depleting C. difficile LDTs leads to loss of 3-3 cross-links and cell death. Our findings establish a new class of bacterial PG cross-linking enzymes and suggest that LDTs might be exploited as selective antibiotic targets for C. difficile.

Author contributions: K.W.B., U.M., D.L.P., D.S.W., and C.D.E. designed research; K.W.B., U.M., R.F.H., D.L.P., and C.D.E. performed research; K.W.B., U.M., K.L.O., A.J.A., M.M.P., and C.D.E. contributed new reagents/analytic tools; K.W.B., U.M., M.M.P., R.F.H., D.L.P., D.S.W., and C.D.E. analyzed data; and K.W.B., U.M., M.M.P., R.F.H., D.L.P., D.S.W., and C.D.E. wrote the paper.

The authors declare no competing interest.

This article is a PNAS Direct Submission

Copyright © 2024 the Author(s). Published by PNAS. This article is distributed under Creative Commons Attribution-NonCommercial-NoDerivatives License 4.0 (CC BY-NC-ND).

<sup>1</sup>Present address: Research & Development, Haleon, Richmond, VA 23220.

 $^2\mbox{To}$  whom correspondence may be addressed. Email: david-weiss@uiowa.edu or craig-ellermeier@uiowa.edu.

This article contains supporting information online at https://www.pnas.org/lookup/suppl/doi:10.1073/pnas. 2408540121/-/DCSupplemental.

Published August 16, 2024.

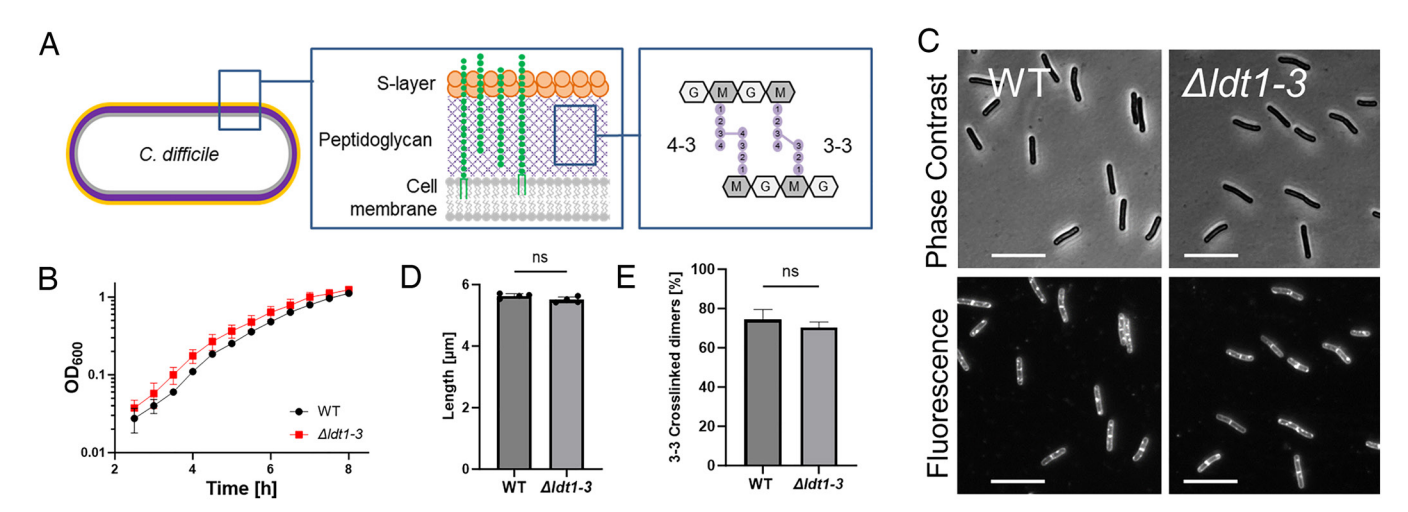


**Fig. 1.** A *C. difficile* mutant lacking all three YkuD-type Ldts ( $\Delta ldt1$ -3) exhibits wild-type growth, morphology, and 3-3 cross-linking. (A) Diagram of the cell envelope of *C. difficile*. The PG matrix contains a repeating disaccharide of NAG (G) and NAM (M). The glycans are cross-linked by short peptides (filled circles) attached to the NAM residues. About 25% of the cross-links are 4-3 cross-links created by PBPs, and 75% are 3-3 cross-links created by LDTs. Polysaccharides (green) analogous to teichoic acids are attached to PG or to a lipid in the cell membrane. (*B*) Growth curve in TY. Filled symbols and error bars indicate the mean ± SD from four biological replicates. (*C*) Phase-contrast and fluorescence micrographs of cells sampled at OD<sub>600</sub> = 0.5 and stained with the membrane dye FM4-64. Size bars, 10 μm. Images representative of 3 experiments. (*D*) Average cell length based on four biological replicates in which >160 cells were measured per sample. Dots depict the mean value from each sample; bars and error bars the mean ± SD across all four trials. ns, not significant in an unpaired two-tailed *t* test. (*E*) Percentage of 3-3 PG cross-links as a fraction of the total cross-linked dimers graphed as mean ± SD from three biological replicates. ns, not significant in an unpaired one-tailed *t* test. Strains used: WT = R20291, Δ*ldt1-3* = KB124.

the  $\varepsilon$ -amino of an mDAP residue in position 3 of an "acceptor" peptide is the attacking nucleophile, leading to formation of a 4-3 peptide cross-link and release of the PBP for further rounds of catalysis. As the name suggests, PBPs are the lethal targets of penicillin and other  $\beta$ -lactam antibiotics, which form a covalent adduct with the active site serine. The enzymes responsible for 3-3 cross-linking are L,D-transpeptidases (LDTs). LDTs are not homologous to PBPs but nevertheless catalyze a similar two-step transpeptidation reaction. Unlike PBPs, LDTs are not known to be essential for viability. Other noteworthy differences include that LDTs are only sensitive to a subset of  $\beta$ -lactams, use a catalytic cysteine rather than a catalytic serine, and require a tetrapeptide rather than a pentapeptide as acyl donor for transpeptidation (12, 19–21).

Peltier et al. reported in 2011 that ~70% of the cross-links in *C. difficile* were 3-3, raising the intriguing possibility that 3-3 cross-linking might be essential for viability of this pathogen (22). All known LDTs contain a YkuD catalytic domain. *C. difficile* encodes three YkuD-domain LDTs, which have been characterized to various degrees both in vivo and in vitro (22–25). Surprisingly, it was recently reported that a *C. difficile* mutant lacking all three LDTs is viable and synthesizes PG with normal levels of 3-3 cross-linking (25). This finding leaves open two major questions: What enzyme(s) catalyze 3-3 cross-linking in the absence of the known YkuD-family LDTs? Does *C. difficile* require 3-3 cross-linked PG for viability?

Here, we show that the "missing" LDTs are two previously uncharacterized VanW domain proteins and that 3-3 cross-links are indeed essential for viability in *C. difficile*. The function of VanW domains was until now unknown, but they are presumed to be involved in vancomycin resistance because they are found in some atypical *Enterococcus* vancomycin resistance gene clusters (26, 27). VanW domains are structurally and evolutionarily unrelated to YkuD domains. Nevertheless, in a remarkable example of convergent evolution, the presence of a conserved and essential cysteine suggests transpeptidation by VanW domains involves a thioacyl enzyme–substrate intermediate, as previously shown for YkuD domains. Our findings can explain how VanW domain

proteins contribute to vancomycin resistance and suggest that LDTs are promising targets for narrow-spectrum antibiotics against *C. difficile*.

#### **Results**

Loss of the Known Ldts Has No Effect on the Level of 3-3 Cross-Links or Cell Viability. All known LDTs contain a catalytic YkuDdomain, which is named after a Bacillus subtilis protein from which one of the first crystal structures was reported (12, 28). C. difficile contains three YkuD-type LDTs (Fig. 2A) (22, 24, 25). To address their contributions to PG biogenesis, we used CRISPR mutagenesis to delete the three *ldt* genes alone and in combination. We had no difficulty constructing a triple deletion strain, referred to here for simplicity as  $\Delta ldt1-3$  even though the genes are not in an operon. We verified the triple mutant by PCR across each *ldt* deletion, western blotting, and whole genome sequencing, which confirmed the three ldt deletions are the only mutations in the strain (SI Appendix, Fig. S1). The  $\Delta ldt1-3$  mutant was not only viable but completely healthy as judged by growth rate, morphology, sensitivity to a collection of cell wall-targeting antibiotics, and muropeptide analysis, which revealed no decrease in 3-3 PG cross-links as compared to the wild-type (Fig. 1 B–E, Tables 1 and 2, and *SI Appendix*, Fig. S2 A and B). Although we were surprised that the known LDTs are not required for 3-3 cross-linking, Galley et al. reported similar results while our study was in progress (25). The fact that 3-3 cross-links are abundant in a  $\Delta ldt1-3$  mutant implies C. difficile must have one or more novel LDT(s).

Bioinformatic Identification of VanW Domain Proteins as Potential LDTs. We reasoned that the missing LDT(s) might be up-regulated to compensate for the absence of the three YkuD-type LDTs, so we used RNA sequencing to compare the gene expression profile of wild-type to  $\Delta ldt1-3$  mutant. The only noteworthy differences were the absence of transcripts for the three ldt genes deleted in the mutant (*SI Appendix*, Fig. S2C and Dataset S1). Although this experiment failed in its original goal of

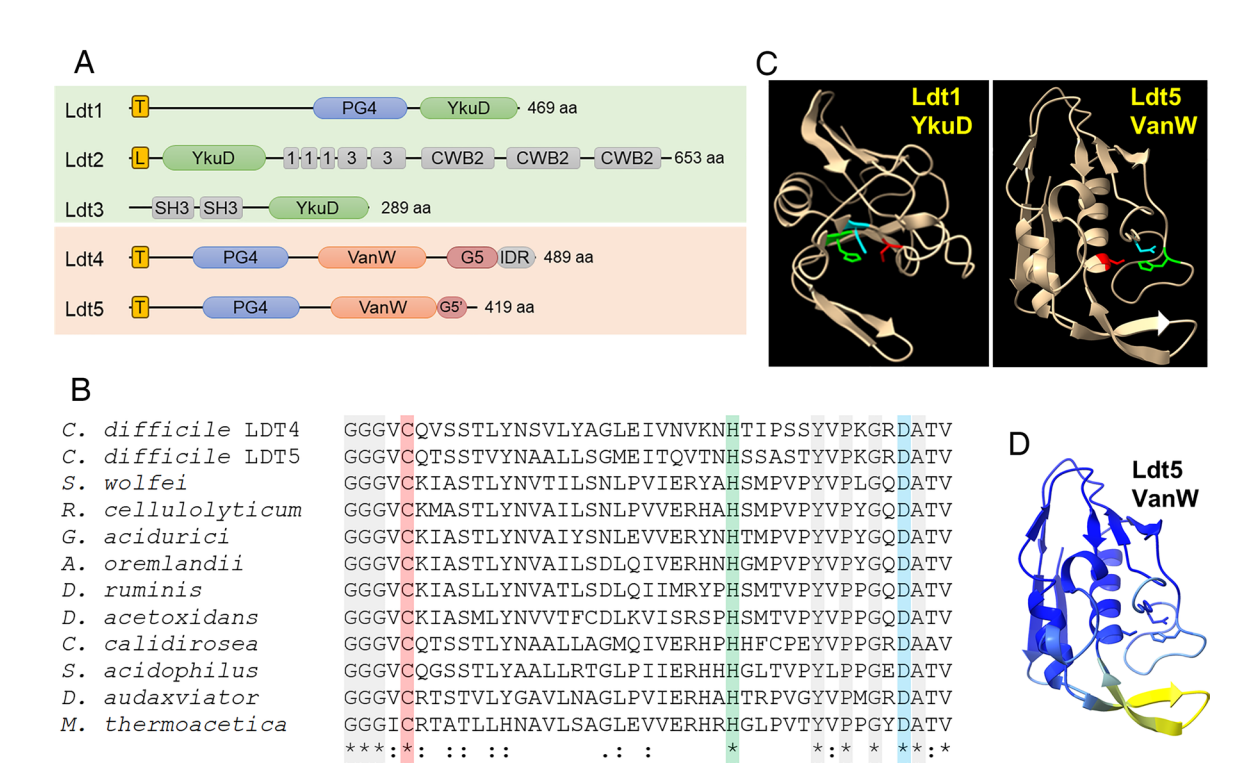


Fig. 2. Predicted structures of C. difficile Ldts. (A) Domain architecture. T, transmembrane helix; L, signal peptidase 2 signal sequence; PG4, PG-binding domain 4; YkuD, L,D-transpeptidase catalytic domain; 1 and 3, choline-binding domains; CWB2, cell wall-binding domain 2; SH3, bacterial SH3 domain; VanW, L,Dtranspeptidase catalytic domain; G5 and G5', complete and partial G5 domains; IDR, intrinsically disordered region. (B) Amino acid sequence alignment of the active site region from 10 VanW domains with the proposed catalytic triad highlighted with red, green, and blue. Gray highlight and asterisks denote strict amino acid identity, colons and periods indicate other conserved positions. Sequences shown are from *C. difficile*, *Desulforudis audaxviator*, *Moorella* thermoacetica, Sulfobacillus acidophilus, Ruminiclostridium cellulolyticum, Gottschalkia acidurici, Alkaliphilus oremlandii, Syntrophomonas wolfei, Desulforamulus ruminis, Desulfofarcimen acetoxidans, and Chthonomonas calidirosea. See SI Appendix, Fig. S1 for an alignment of the entire VanW domains. (C) AlphaFold2 models of the YkuD-domain from C. difficile Ldt1 and the VanW domain from Ldt5, with the catalytic triads in color: Cys (red), His (green), Asp (cyan). (D) Confidence of the Ldt5 VanW domain model based on predicted local distance difference test. Dark blue >90 (highly accurate), light blue 89-70 (modeled well), and yellow 69-50 (low confidence, caution).

finding the missing LDT(s), the absence of a cell envelope stress response underscores the basic health of the  $\Delta ldt1-3$  mutant.

We then searched the C. difficile R20291 genome in BioCyc (29) for proteins with the noncatalytic domains annotated in the various C. difficile LDTs (Fig. 2A). Hits to the choline-binding, cell wall-binding, and bacterial SH3 domains in Ldt2 and Ldt3 returned proteins that were either unlikely candidates for an LDT (e.g., PG hydrolases and the major toxins TcdA and TcdB) or too numerous to test (e.g., 27 proteins with the cell wall-binding 2 domain). In contrast, a search with the PG\_binding\_4 domain

(PG4; PF12229) found in Ldt1 only returned two uncharacterized proteins, CDR20291\_1285 and CDR20291\_2055, which we have named Ldt4 and Ldt5 based on results shown below. Interestingly, all three *C. difficile* PG4 domain proteins (i.e., Ldt1, Ldt4, and Ldt5) are up-regulated in a mutant lacking the PrkC serine/threonine kinase involved in cell envelope homeostasis (30), suggesting a shared function.

Both Ldt4 and Ldt5 are predicted membrane proteins with large extracellular domains that include a PG4 domain and a VanW domain (PF04294) (Fig. 2A). In Ldt4, the VanW domain

Table 1. Muropeptide quantitation

			Peak area [%]*								
Peak <sup>†</sup>	Muropeptide <sup>‡</sup>	3-3 <sup>§</sup>	WT	Δ1-3	Δ4Δ5	Δ1-3Δ4	Δ1-3Δ4 P <sub>tet</sub> ::ldt5	Ave Rt <sup>¶</sup> [min]	Calculated monoisotopic mass (+H)	Observed monoisotopic mass (+H)	
1	DS-TriP		6.9 ± 0.7	8.5 ± 0.4	5.3 ± 1.1	6.2 ± 1.4	1.6 ± 0.0	10.9	829.36730	829.3656	
1a	DS-TriP		$2.8 \pm 0.3$	1.9 ± 0.1	$3.3 \pm 0.2$	$2.8 \pm 0.3$	$7.4 \pm 2.3$	12.6	829.36730	829.3651	
4	DS-TriP-Gly		$5.9 \pm 0.0$	$2.3 \pm 0.0$	$5.6 \pm 0.3$	$2.3 \pm 0.1$	$0.2 \pm 0.1$	14.8	886.38876	886.3864	
7	DS-TetraP		35.7 ± 1.9	$38.8 \pm 0.4$	43.8 ± 1.6	41.7 ± 1.4	$68.0 \pm 0.9$	19.5	900.40441	900.4022	
15a	DS-TriP-TetraP-DS	Υ	27.6 ± 1.8	25.5 ± 0.1	23.2 ± 1.9	$24.9 \pm 0.8$	3.7 ± 1.1	40.6	1,710.75387	1,710.7486	
17	DS-TriP-TetraP-DS	Υ	$6.9 \pm 0.1$	$7.3 \pm 0.0$	$4.3 \pm 0.2$	$6.8 \pm 0.4$	$0.9 \pm 0.2$	44.3	1,710.75387	1,710.7484	
19	DS-TetraP-TetraP-DS	Ν	$9.8 \pm 0.5$	$10.8 \pm 0.3$	$9.8 \pm 0.5$	10.6 ± 0.2	11.8 ± 1.2	46.0	1,781.79099	1,781.7849	
21	DS-TetraP-TetraP-DS	N	$4.3 \pm 0.2$	4.9 ± 0.3	$4.7 \pm 0.2$	$4.8 \pm 0.1$	$6.5 \pm 0.3$	49.5	1,781.79099	1,781.7849	

<sup>\*</sup>Values are averages and SD for three independent samples.

†Peaks numbered as in ref. 22.

<sup>&</sup>lt;sup>‡</sup>All disaccharides (DS) are deacetylated.

<sup>3-3</sup> cross-links; Y: yes, N: no. Average retention time.

Table 2. PG cross-linking

	WT	Δ1-3	$\Delta 4 \Delta 5$	$\Delta 1-3\Delta 4$	Δ1-3Δ4 P <sub>tet</sub> ::ldt5
% DS* in monomers	51	52	58	53	77
% DS in dimers	49	48	42	47	23
% DS 3-3 cross-linked	35	33	28	32	5
% DS 4-3 cross-linked	14	16	15	15	18
% dimers 3-3 cross-linked	71	68	65	67	20
% dimers 4-3 cross-linked	29	32	35	33	80

<sup>\*</sup>DS: disaccharides.

is followed by a G5 domain (PF07501) and an intrinsically disordered region (IDR). Ldt5 appears to have the first half of a G5 domain (G5'). PG4 domains are often found in YkuD-type LDTs and have been proposed to bind PG (31), but PG-binding has not been demonstrated. G5 domains are named for conserved glycines. They are found in many extracellular proteins from gram-positive organisms (31), bind zinc and heparin (32, 33), and have been modeled into the structure of PG (34), but there is no experimental evidence for PG-binding. C-terminal IDRs in PBPs are proposed to target these enzymes to gaps in the sacculus to make repairs (35).

No function has been proposed for VanW domains, which were first recognized in atypical Enterococcus vancomycin resistance gene clusters (26, 27). Close inspection of VanW domain sequence alignments revealed a conserved cysteine, histidine, and aspartate that are positioned to form a catalytic triad when mapped onto the high-confidence AlphaFold2 (AF2) (36) models of the VanW domains from Ldt4 and Ldt5 (Fig. 2 B-D and SI Appendix, Figs. S3 and S4). Similar triads are found in YkuD-type LDTs (modeled for C. difficile Ldt1 in Fig. 2C), which catalyze a two-step transpeptidation reaction via a covalent thioacyl-enzyme intermediate (12, 37, 38). Despite this similarity, VanW and YkuD domains have different folds and cannot be superimposed. Moreover, searches with DALI and Foldseek indicate the VanW domain has no significant similarity to any known structures (39-41). Thus, the VanW domain appears to represent a novel fold with a catalytic triad as found in YkuD-family LDTs.

VanW Domain Proteins Ldt4 and Ldt5 are LDT In Vitro. Transpeptidase activity can be assayed by monitoring incorporation of fluorescent substrate analogs into isolated PG sacculi (42). We purified the soluble extracellular domains of Ldt4, Ldt5, and as a control the YkuD-domain protein Ldt1 (Ldt4<sup>28-489</sup>, Ldt5<sup>38-419</sup>, Ldt1<sup>39-469</sup>) (SI Appendix, Fig. 55A). The enzymes were tested using TetraRh, a fluorescent analog of an authentic LDT acyl donor substrate (43). TetraRh consists of a Rhodamine dye attached to the N terminus of a tetrapeptide based on Enterococcus faecium PG with the sequence: D-Ala-iso-D-Gln-L-Lys(Ac)-D-Ala (Fig. 3A and SI Appendix, Fig. S6). Note that the Lysine is acetylated to prevent it from acting as a transpeptidation acceptor. To test for LDT activity, enzyme and TetraRh were incubated with B. subtilis PG sacculi that had been immobilized on a glass slide. After 1 h, the sacculi were washed and imaged by phase-contrast and fluorescence microscopy. The results are compiled in Fig. 3B. All three LDTs incorporated TetraRh into sacculi, although fluorescence was about fourfold higher with Ldt1 than Ldt4 or Ldt5 (Fig. 3C). In contrast, none of the LDTs incorporated label when D-Ala in TetraRh was replaced with L-Ala, nor did they incorporate a pentapeptide analog (PentaRh) that is a substrate for PBPs but not LDTs (43). As expected, changing the active site cysteine to alanine in Ldt4 and Ldt5 abrogated activity with TetraRh. Circular dichroism spectra of the Ldt4<sup>C286A</sup> and Ldt5<sup>C298A</sup> mutant proteins were indistinguishable from WT, indicating they folded properly (*SI Appendix*, Fig. S5*B*). Finally, meropenem inhibited the activity of Ldt1, Ldt4, and Ldt5 (Fig. 3*D*). Inhibition of Ldt1 was expected as meropenem is known to acylate this enzyme (24). Inhibition of Ldt4 and Ldt5 argues that VanW domains and YkuD domains have very similar active sites, which has implications for developing antibiotics effective against both LDT families.

We next tested Ldt4 and Ldt5 for L,D-transpeptidase activity using disaccharide-tetrapeptide (DS-TetraP) isolated by highperformance liquid chromatograph (HPLC) after mutanolysin digestion and borohydride reduction of purified C. difficile PG sacculi. DS-TetraP has the structure NAG-NAM(red)-L-Ala-iso-D-Glu-meso-DAP-D-Ala, with the NAM moiety in the muramitol form due to the reduction step. Reaction mixtures containing enzyme and DS-TetraP were incubated for 2 h at 37 °C and then analyzed by HPLC. Ldt4 and Ldt5 converted DS-TetraP to a product with a retention time of 31 min (Fig. 3E), which was determined by elution time and mass spectrometry to be disaccharide-tripeptide 3-3 cross-linked to a disaccharide-tetrapeptide (DS-TriP-TetraP-DS) (SI Appendix, Fig. S7). Ldt1, Ldt4, and Ldt5 all exhibited carboxypeptidase activity, producing a product with retention time of 21 min, which was determined by elution time and mass spectrometry to be DS-TriP. As expected, the catalytic mutant derivatives Ldt4<sup>C286A</sup> and Ldt5<sup>C298A</sup> were unable to produce a cross-linked product, although both generated some DS-TriP, indicating they retain carboxypeptidase activity (Fig. 3*E*). We interpret these results to mean that the catalytic cysteine is required for transpeptidation, presumably because of its role as an acyl carrier, but other features of the enzyme that promote catalysis such as transition state stabilization are sufficient for removal of the terminal D-Ala<sup>4</sup>. Of note, but in agreement with a previous study (24), Ldt1 did not cross-link DS-TetraP in our assay, although Ldt1 has been shown to generate a small amount of cross-linked product by using more enzyme and longer incubations (25). The fact that Ldt1 has little or no ability to cross-link DS-TetraP yet outperforms Ldt4 and Ldt5 for incorporation of TetraRh into intact sacculi suggests it requires a substrate larger than a DS-TetraP as acceptor in the transpeptidation reaction.

#### LDTs and 3-3 Cross-Links Are Essential for Viability in C. difficile.

Having determined that the VanW domain proteins are bona fide LDTs, we addressed their contribution to 3-3 cross-linking in vivo. To this end, we used CRISPR mutagenesis to create the  $\Delta ldt4$ ,  $\Delta ldt5$ , and  $\Delta ldt4\Delta ldt5$  strains. All of these mutants were viable and exhibited typical rod morphology (Fig. 4A and SI Appendix, Fig. S8A). In addition, muropeptide analysis of the  $\Delta ldt4\Delta ldt5$  strain revealed normal levels of 3-3 cross-linking (Fig. 5A and Tables 1 and 2). We then deleted either ldt4 or ldt5 in the  $\Delta ldt1-3$  background. Once again the mutants were viable with no change in morphology (Fig. 4A and SI Appendix, Fig. S8A), and the  $\Delta ldt1-3\Delta 4$  strain retained normal levels of 3-3 cross-linking (Fig. 5A and Tables 1 and 2). We also tested whether sporulation was affected in some of the mutants

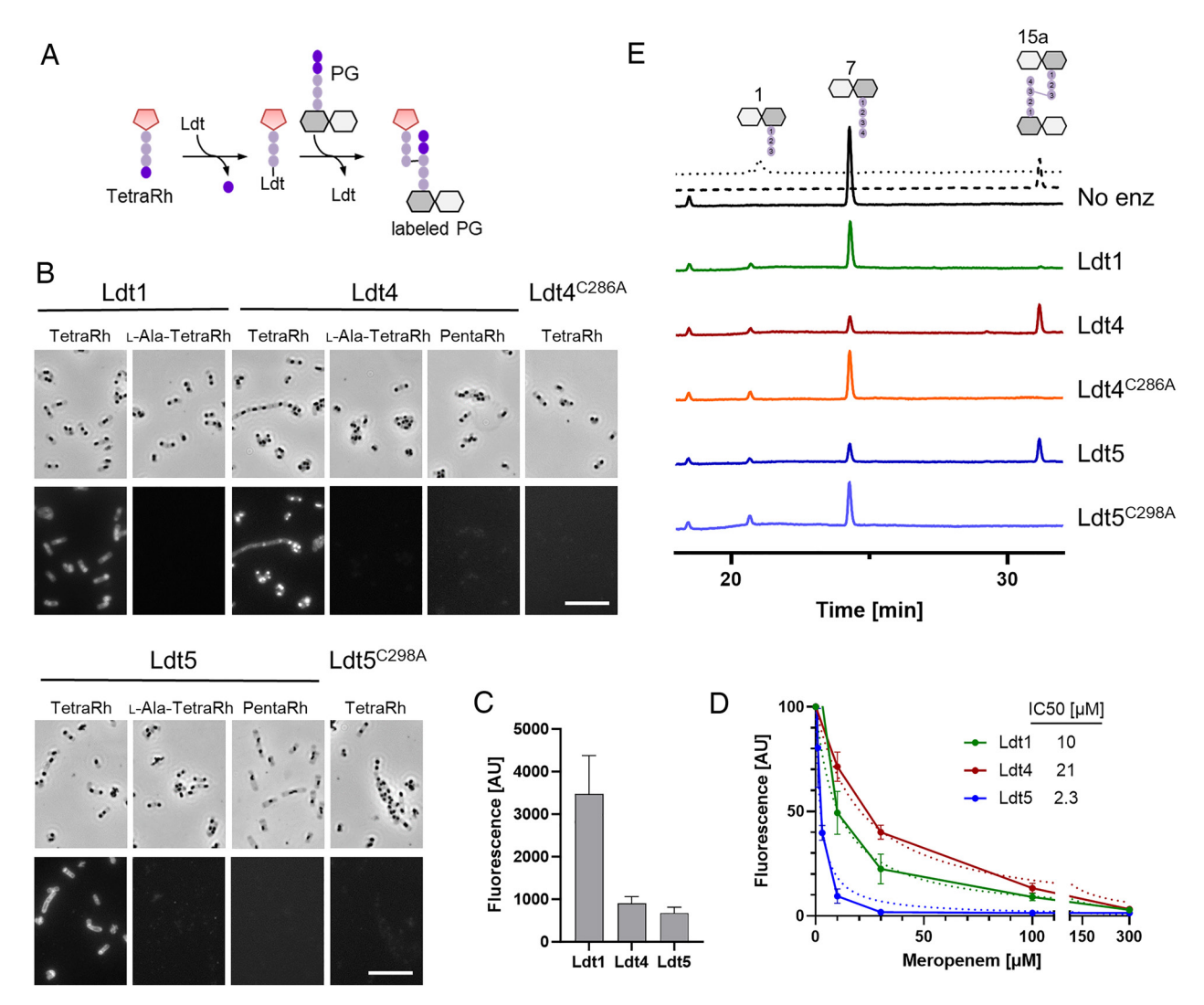


Fig. 3. VanW domains catalyze L,D-transpeptidation in vitro. (A) Schematic diagram of incorporation of TetraRh into PG sacculi by an Ldt. Pink pentagon, Rhodamine. Colored balls, amino acids. Dark and light gray hexagons, NAM and NAG, respectively. (B) Phase-contrast and fluorescence micrographs of immobilized PG sacculi after incubation for 1 h with 5 μM enzyme and 30 μM substrate analog as indicated. TetraRh: LDT-specific substrate analog; L-Ala-TetraRh, negative control; PentaRh, PBP-specific substrate. Size bar, 10 µm. Micrographs are representative of at least two experiments. (C) Quantification of TetraRh incorporation into sacculi graphed as the mean ± SD of the fluorescence intensity from 10 sacculi. (D) Inhibition of LDT activity by meropenem graphed as the mean and SD of data pooled from four experiments. IC50 is the concentration of meropenem needed to reduce LDT activity by half. (E) HPLC analysis of muropeptides after 1 h incubation of the indicated enzymes with DS-TetraP substrate. Structures above the chromatograms are numbered according to Peltier et al. (22). Calibration traces for 1 and 15a are shown by the dotted and dashed lines, respectively. Chromatograms are representative of three experiments

and observed a modest increase in some cases (SI Appendix, Fig. S8B). However, multiple attempts to delete all five *ldt*s were unsuccessful, suggesting a synthetic lethal phenotype. This was confirmed using CRISPRi to knock down expression of ldt4 in a  $\Delta ldt1-3\Delta 5$  mutant or ldt5 in a  $\Delta ldt1-3\Delta 4$  mutant. In both cases, knockdown of the last remaining LDT caused a 2 to 3 log drop in viability (SI Appendix, Fig. S9)

We then replaced the native promoter for ldt5 with P<sub>tet</sub> in the  $\Delta ldt 1-3\Delta 4$  background, rendering expression of the last remaining LDT dependent on the inducer anhydrotetracycline (aTet). Spot titer assays on tryptone-yeast (TY) media with and without aTet revealed Ldt5 was required for viability (Fig. 4A). This result was confirmed in liquid media, where subculturing into TY lacking aTet resulted in slower growth and eventually a drop in OD<sub>600</sub> indicative of lysis (Fig. 4B). Microscopy revealed cells depleted of the last remaining LDT became longer, thinner, and curvy in comparison to WT. Cell ghosts indicative of lysis were also seen (Fig. 4 C and D). Staining with the membrane dye FM4-64 revealed relatively few division septa in the population depleted

of LDTs (Fig. 4C). These phenotypic defects implicate LDTs in elongation and cell division.

To determine whether the viability loss is associated with the loss of 3-3 cross-links, we analyzed muropeptides from WT, the  $\Delta ldt 4\Delta ldt 5$  double mutant, the  $\Delta ldt 1-3\Delta 4$  quadruple mutant, and the  $\Delta ldt 1-3\Delta 4$  P<sub>tet</sub>::ldt5 depletion strain. Cultures were grown in TY, which was supplemented with a small amount of aTet (0.25 ng/mL) for the depletion strain so it could reach high enough  $OD_{600}$ to obtain sufficient sacculi for muropeptide analysis. Muropeptides were identified by mass spectrometry and named according to Peltier et al. to facilitate comparisons (Fig. 5A) (22). There was a drastic reduction in muropeptides 1, 4, 15a, and 17 in the depletion strain. All of these changes are attributable to loss of LDT activity. Most importantly, peaks 15a and 17 are two 3-3 cross-linked DS-TriP-TetraP-DS species that separate during HPLC for unknown reasons. The area under the curve for muropeptides 15a+17 decreased from 34.5 in WT to 4.6% in the depletion strain, an ~85% decrease (Tables 1 and 2). Peaks 1 and 4 are DS-TriP and DS-TriP-Gly, which are created by LDT-catalyzed carboxypeptidase and exchange

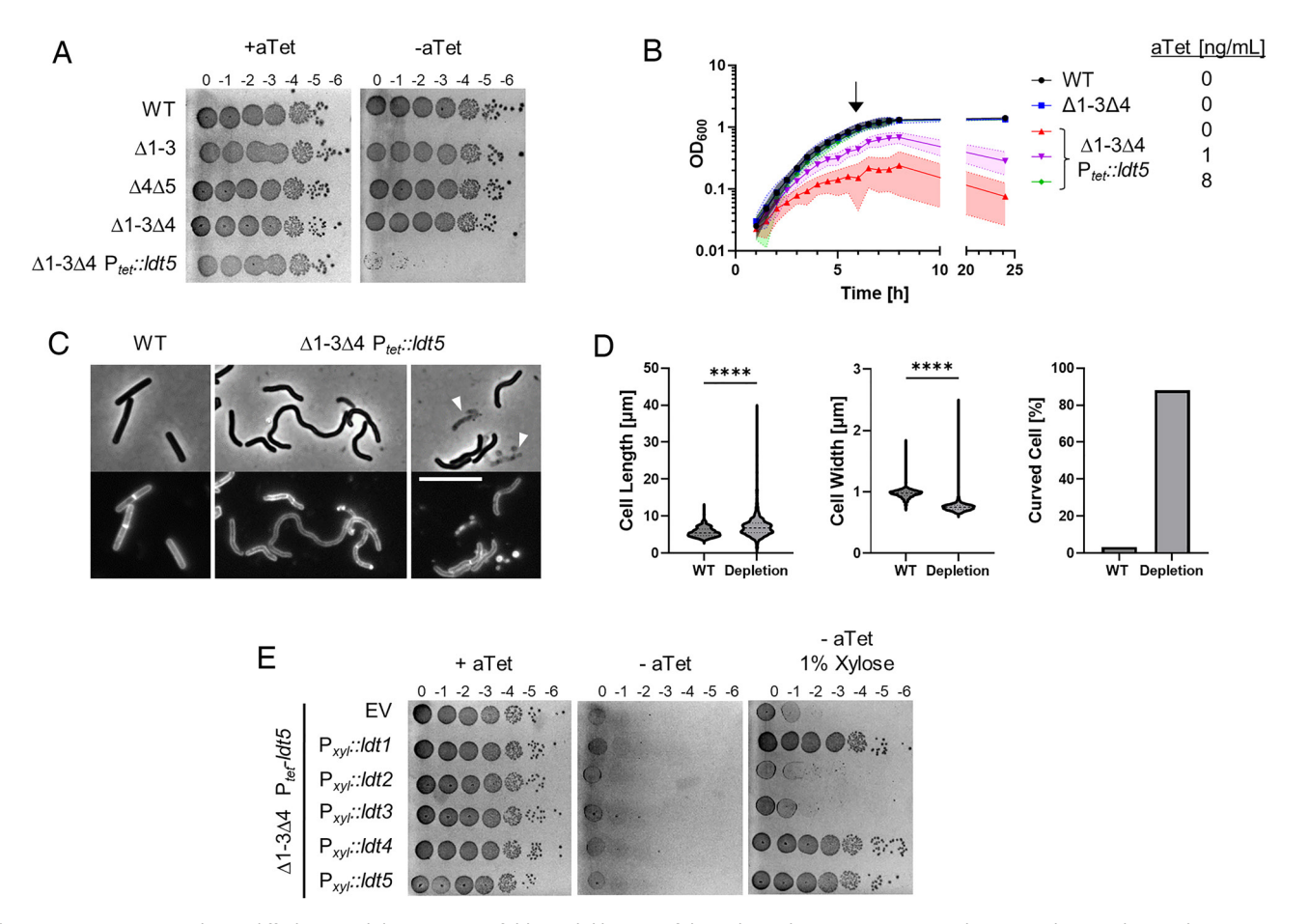


**Fig. 4.** LDTs are essential in *C. difficile*. (*A*) Viability assay. Tenfold serial dilutions of the indicated strains were spotted onto TY plates with or without 25 ng/mL aTet. Plates were photographed after incubation for 18 h. Images are representative of at least three experiments. (*B*) Growth curves. Data are graphed as the mean ± SD of four biological replicates from different days. (*C*) Cell morphology. Cells grown for 6 h in TY without aTet (arrow in *B*) were stained with the membrane dye FM4-64 and photographed under phase-contrast and fluorescence microscopy. Arrowheads indicate lysed cells. Size bar, 10 μm. Images representative of at least three experiments. (*D*) Quantification of length, width, and shape based on 781 cells of WT and 1,196 cells of the depletion strain pooled from three biological replicates. Cells with a sinuosity score ≥1.03 were considered curved. \*\*\*\*P < 0.0001, unpaired t test. (*E*) Complementation assay. Tenfold serial dilutions of the LDT depletion strain harboring the indicated expression plasmids were spotted onto TY with or without 25 ng/mL aTet and 1% xylose. Plates were photographed after incubation for 18 h. Images are representative of three biological replicates. Strains shown in A-D: WT, R20291;  $\Delta$ 1-3, KB124;  $\Delta$ 4 $\Delta$ 5, KB529;  $\Delta$ 1-3 $\Delta$ 4, KB474;and  $\Delta$ 1-3 $\Delta$ 4 P<sub>tet</sub>::ldt5, KB547 (called "depletion" in panel *D*). Strains shown in panel *E*: empty vector (EV), KB548, P<sub>xyi</sub>::ldt1, KB549; P<sub>xyi</sub>::ldt2, KB550; P<sub>xyi</sub>::ldt3, KB551; P<sub>xyi</sub>::ldt4, KB552; and P<sub>xyi</sub>::ldt5, KB553.

reactions, respectively. A minor DS-TriP species eluting as peak 1a appears to be increased in the depletion stain; we cannot at present explain that change. Interestingly, loss of 3-3 cross-linking increased primarily uncross-linked muropeptides (Peaks 1a and 7) rather than 4-3 cross-linking muropeptides (Peaks 19 and 21). Thus, LDTs and PBPs are not in competition, which can be explained by their different acyl donor requirements, and *C. difficile* is unable to compensate for defects in 3-3 cross-linking by making more 4-3 cross-links instead.

We further characterized LDTs in vivo using TetraRh (Fig. 5B). Flow cytometry of wild-type C. difficile cells grown for 1 h in the presence of 30  $\mu$ M TetraRh revealed a ~350-fold increase in fluorescence as compared to background determined using the non-physiological L-Ala-TetraRh variant. Label incorporation decreased ~30-fold in the  $\Delta ldt1-3$  strain but was unaffected in the  $\Delta ldt4\Delta ldt5$  strain, indicating TetraRh is a much better substrate for C. difficile's YkuD-type LDTs than for its VanW-type LDTs, as was seen in vitro (Fig. 3 B and C). Deletion of ldt4 in the  $\Delta ldt1-3$  background further reduced TetraRh incorporation, but deletion of ldt5 had little effect. Finally, labeling with TetraRh dropped to near background when the  $\Delta ldt1-3\Delta 4$  P<sub>tet</sub>::ldt5 depletion strain was grown without aTet (Fig. 5B). Overall, experiments

with TetraRh confirm the absence of LDT activity in the  $\Delta ldt 1-3\Delta 4$  P<sub>trt</sub>::ldt 5 depletion strain.

**Ldt1, Ldt4, or Ldt5 Is Sufficient for Viability.** The above results demonstrate C. difficile must express at least one *ldt* for 3-3 cross-linking and viability. But which one(s)? To address this question, we cloned each *ldt* into a plasmid with a xylose-inducible promoter,  $P_{xyl}(44)$ . The resulting *ldt* expression plasmids were conjugated into the  $\Delta ldt1$ - $4P_{tet}$ ::*ldt5* depletion strain, and viability was determined by a spot titer assay on TY with 1% xylose but no aTet. We found that Ldt1, Ldt4, or Ldt5 were each sufficient for viability, but Ldt2 or Ldt3 were not (Fig. 4E), even though they were produced at physiological levels or higher as determined by western blotting (*SI Appendix*, Fig. S1 *B–D*). Moreover, CRISPRi knockdown of *ldt1* in a  $\Delta ldt4$ - $\Delta mutant$  resulted in a loss of viability, indicating that Ldt2 and Ldt3 are not sufficient for normal growth even when present simultaneously (*SI Appendix*, Fig. S9).

VanW Domain Containing Proteins Are Common in Gram-Positive Bacteria. The Pfam database (v31, November 2023) lists 15,131 VanW domain proteins from 6,920 bacterial species (45). That makes VanW domains almost 10-fold less common than

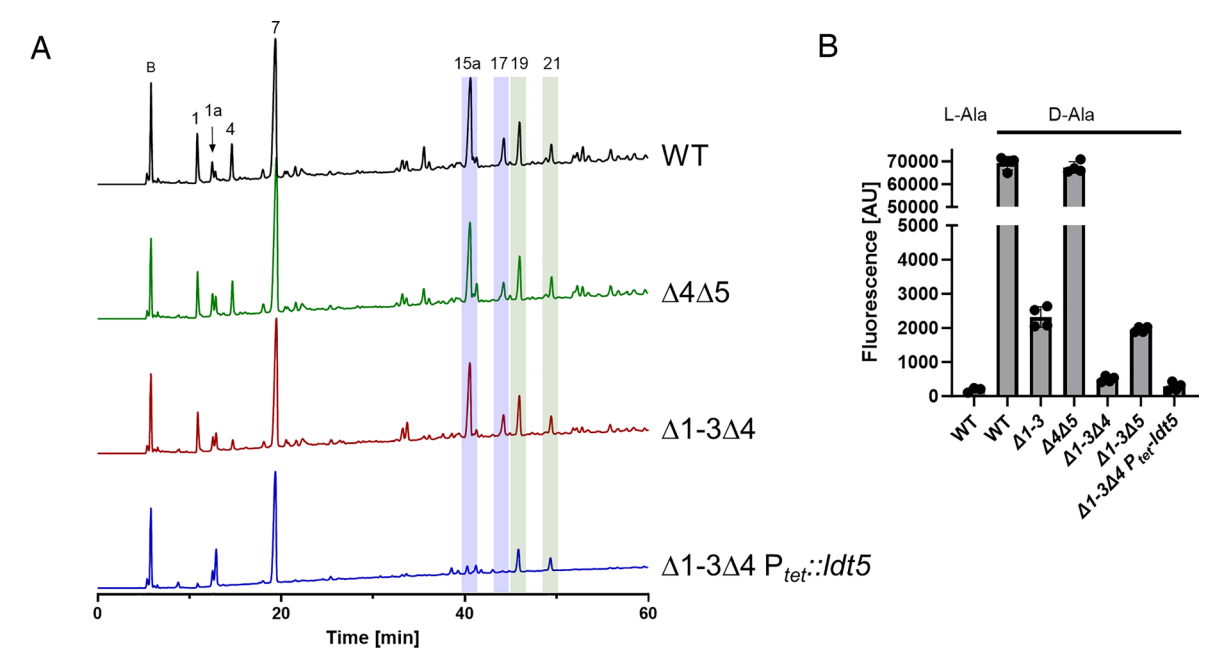


Fig. 5. YkuD and VanW LDTs create 3-3 cross-links in vivo. (A) HPLC quantitation of muropeptides from the indicated strains. Blue and green highlights indicate the major 3-3 and 4-3 cross-linked muropeptides, respectively. Peak numbers based on ref. 22. (B) Flow cytometry analysis of cells grown for 1 h in the presence of TetraRh. L-Ala is a control and refers to a nonphysiological TetraRh analog with L-alanine rather than D-Ala in position 4. Strains: WT, R20291;  $\Delta 4\Delta 5$ , KB529;  $\Delta$ 1-3 $\Delta$ 4, KB474;  $\Delta$ 1-3 $\Delta$ 4 P<sub>tet</sub>::Idt5, KB547;  $\Delta$ 1-3, KB124; and  $\Delta$ 1-3 $\Delta$ 5, KB502.

YkuD domains, for which Pfam lists about ~131,000 examples in ~30,000 bacterial species. About half of the VanW domain proteins have one or more PG4 domains, as seen in Ldt4 and Ldt5 of C. difficile. Using AnnoTree (46) to map the Pfam VanW domains onto a bacterial phylogenetic tree revealed a patchy distribution with ~70% of Bacillota (formerly called Firmicutes) and ~40% of Actinomycetota having at least one predicted VanW domain protein (Fig. 6A). Indeed, these two phyla account for ~65% of all sequenced VanW homologs. In contrast, only ~10% of Cyanobacteria, 6% of Bacteroidota, and 1% of Pseudomonadota genomes encode a predicted VanW domain protein. VanW domains are notably absent from *E. coli*, *Salmonella typhimurium*, Caulobacter crescentus, Staphylococcus aureus, and Streptococcus pneumoniae. B. subtilis and some (but not all) Enterococcus faecalis strains have a VanW domain protein, but these have not been characterized. Not enough is known about the structure of PG

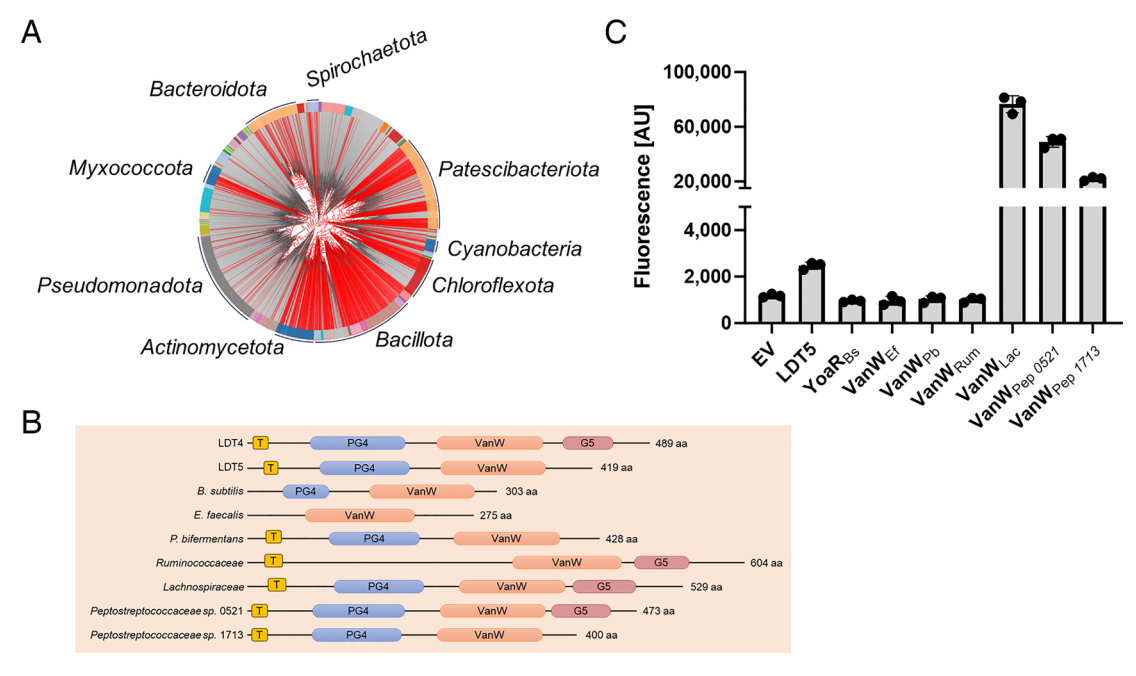


Fig. 6. VanW domain LDTs are most prevalent in gram-positive bacteria. (A) Phylogenetic distribution of VanW domains (red lines). Some phyla names were pruned for clarity. (B) Domain structure of VanW domain proteins tested for LDT activity. Domains labeled as in Fig. 14. (C) Flow cytometry analysis of cells grown for 1 h in the presence of TetraRh graphed as the mean  $\pm$  SD from three trials. The strains are derivatives of KB474 [ $\Delta ldt^{1}$ - $3\Delta ldt^{4}$ ] harboring  $P_{xyl}$  expression vectors: EV, KB633; C. difficile Ldt5, KB634; B. subtilis YoaR, KB635; E. faecalis VanW, KB636; Paraclostridium bifermentans VanW, KB637; Ruminococcaceae sp. VanW, KB638; Lachnospiraceae sp. VanW, KB639; Peptostreptococcus sp. VanW 0521, KB640; and Peptostreptococcus sp. VanW 1713, KB 641.

in different bacteria to comment on whether VanW domains are overrepresented in bacteria where 3-3 cross-links are more abundant.

We used TetraRh to test seven foreign VanW domain proteins for LDT activity when expressed from a  $P_{xyl}$  plasmid in a C. difficile strain deleted of all LDTs except Ldt5 (Fig. 6B). This strain grows well but Ldt5 does not incorporate TetraRh very efficiently so background fluorescence is low. Three of the seven foreign VanW domain proteins supported robust incorporation of TetraRh into C. difficile, confirming that they are LDTs (Fig. 6C). The four VanW domain proteins that failed to incorporate TetraRh are difficult to interpret—they might not have been expressed, they might require different assay conditions, or they might not be LDTs.

### **Discussion**

Most bacteria rely primarily on PBPs that make 4-3 cross-links to construct an osmotically stable PG wall. C. difficile, in contrast, relies primarily on 3-3 cross-links created by LDTs (22). We have demonstrated that 3-3 cross-linking and LDTs are essential for viability in C. difficile, making it so far the only bacterium in which 3-3 cross-links and LDTs are known to be essential. We also report the identification of a family of LDTs whose hallmark is a VanW catalytic domain, which has no sequence or structural similarity to the YkuD catalytic domain found in all previously known LDTs (12). Indeed, VanW domains appear to represent a novel fold, as searches to detect related structures using Foldseek (39) or remote homologs using HHsearch (47) did not return any statistically significant matches. Nevertheless, we infer that VanW and YkuD domains catalyze 3-3 cross-linking by a similar two-step catalytic mechanism based on the presence of a conserved cysteine that is required for transpeptidation. In YkuD domains, this cysteine is the attacking nucleophile that forms a covalent thioacyl intermediate with the donor peptide substrate (20, 37, 48).

VanW domains are named for their presence in atypical Enterococcus vancomycin resistance gene clusters (26, 27). There is no experimental evidence for a role in vancomycin resistance, nor has any biochemical function been proposed. The finding that VanW domains catalyze 3-3 cross-linking suggests a mechanism by which they could contribute to vancomycin resistance. Vancomycin inhibits PG synthesis by binding to the terminal D-alanyl-D-Ala of the pentapeptide in PG precursors. Known resistance mechanisms involve modifying the stem peptide to prevent vancomycin binding by changing the terminal D-Ala to D-serine or D-lactate (49, 50), or by converting pentapeptides to tetrapeptides that are subsequently cross-linked by LDTs (51). But the latter resistance mechanism comes at a cost because it renders the PBPs inoperative. Curiously, C. difficile is vancomycin sensitive despite its heavy reliance on LDTs for PG cross-linking (22, 52). Further work will be needed to understand this conundrum, but it could have to do with the fact that C. difficile has two PBPs that are essential for vegetative growth. Alternatively, or in addition, vancomycin might block conversion of pentapeptides to tetrapeptides by extracellular carboxypeptidases and thus starve LDTs of substrate. Similarly, dual inhibition of synthetic PBPs and carboxypeptidases might explain why C. difficile is sensitive to  $\beta$ -lactams like ampicillin that do not inhibit LDTs directly (53).

In considering the potential advantages of LDTs over PBPs in PG biogenesis, an important distinction is that only LDTs can repair broken cross-links in the absence of de novo PG synthesis (17). In particular, endopeptidase cleavage of a 4-3 cross-link generates tetra- and tripeptides that can be stitched back together as a 3-3 cross-link by an LDT but not a PBP. The repair function of

LDTs is important for maintaining PG integrity in *Mycobacterium smegmatis* and presumably other bacteria that exhibit polar growth and high levels of 3-3 cross-linking (17). However, we hypothesize that *C. difficile* employs LDTs as the major source of initial cross-linking during elongation and perhaps division as well. Using the fluorescent D-amino acid HADA to visualize sites of PG synthesis in growing *C. difficile* cells revealed uniform incorporation throughout the sidewall, arguing against polar growth (54). Moreover, the primary morphological defects we observed upon LDT depletion—longer, thinner, curvy cells with few septa—are more suggestive of a PG synthesis defect than a repair defect, which should have manifested as bloating and bulges, as reported in *M. smegmatis* (17).

The unique essentiality of 3-3 cross-links in *C. difficile* suggests LDTs might be explored as targets for antibiotics that kill *C. difficile* without disrupting the normal intestinal microbiota needed to keep *C. difficile* in check. Previous efforts to develop antibiotics that inhibit LDTs have focused mainly on *Mycobacterium tuberculosis* Ldt<sub>Mt2</sub>, which is required for virulence but not for viability per se (55, 56). These efforts have mostly been directed at improving the efficacy of penems and carbapenems (48, 57, 58). However, penems and carbapenems also inactivate PBPs. This may be a plus for treating tuberculosis but compromises the selectivity that makes LDTs attractive therapeutic targets in *C. difficile*. Nevertheless, our finding that meropenem inhibits *C. difficile*'s YkuD and VanW domain LDTs argues that it is possible to develop drugs that target both classes of LDTs despite their profoundly different structures.

#### **Materials and Methods**

Strains, Media, and Growth Conditions. Bacterial strains are listed in SI Appendix, Table S1. C. difficile strains used in this study were all derived from R20291 (59). C. difficile was grown in TY medium, supplemented as needed with thiamphenicol at  $10~\mu g/mL$  (Thi $_{10}$ ), kanamycin at  $50~\mu g/mL$ , or cefoxitin at  $8~\mu g/mL$ . Anhydrous tetracycline (aTet) was used to induce genes under  $P_{tet}$  control (Fluka). TY medium consisted of 3% tryptone, 2% yeast extract, and 2% agar (for solid medium). For conjugation plates, brain heart infusion (BHI, Bacto) solid medium was used. BHI media consisted of 3.7% BHI and 2% agar. C. difficile strains were grown at 37 °C in an anaerobic chamber (Coy Laboratory Products) in an atmosphere of about 2%  $H_2$ , 5%  $CO_2$ , and 93%  $N_2$ . Growth was monitored at  $OD_{600}$  with a WPA Biowave CO8000 Cell Density Meter.

 $\it E.~coli$  and  $\it B.~subtilis$  strains were grown in lysogeny broth (LB) medium at 37 °C with chloramphenical at 10 μg/mL or ampicillin at 100 μg/mL as necessary. LB contained 1% tryptone, 0.5% yeast extract, 0.5% NaCl, and 1.5% agar (for solid medium).

Fluorescent Substrate Analogs. The L,D-transpeptidase specific substrate analog, Rhodamine-L-Ala-iso-D-Gln-L-Lys(Ac)-D-Ala (TetraRh), the negative control, Rhodamine-L-Ala-iso-D-Gln-L-Lys(Ac)-L-Ala (L-ala-TetraRh) and the PBP-specific substrate analog, Rhodamine-L-Ala-iso-D-Gln-L-Lys(Ac)-D-Ala-D-Ala (PentaRh) were synthesized as described (43) (SI Appendix, Fig. S6).

Plasmid and Bacterial Strain Construction. Plasmids are listed in SIAppendix, Table S2, and were constructed by isothermal assembly with reagents from New England Biolabs (Ipswich, MA). Regions that were constructed by PCR were verified by DNA sequencing. The oligonucleotide primers used in this study were synthesized by Integrated DNA Technologies (Coralville, IA) and are listed in SIAppendix, Table S3. All plasmids were propagated using OmniMax 2-T1R as the cloning host. Conjugation into C. difficile used either E. coli HB101/pRK24 or B. subtills BS49 as donor (60-63). CRISPR editing plasmids were designed as previously described (63, 64) with a single guide RNA against the target gene and homology regions to repair the double-stranded break caused by the Cas9 nuclease. Successful mutagenesis was confirmed by PCR with Q5 or Taq DNA polymerase (New England Biolabs). Detailed procedures for strain construction are provided in SIAppendix.

Whole-Genome and RNA Sequencing. Samples were prepared and analyzed mostly as described (65, 66). Details are provided in SI Appendix.

Antibiotic Minimum Inhibitory Concentration Determination. The minimum inhibitory concentration against select antibiotics was determined as described in biological duplicate on two separate days (62). Briefly, overnight cultures were diluted 1:100 into TY, grown to  $OD_{600} \sim 0.8$  and then diluted to a calculated  $OD_{600} =$ 0.005 (~ $10^6$  CFU/mL). A 50  $\mu$ L aliquot of cells was added to 50  $\mu$ L of TY plus antibiotic in 96-well plates. Growth was scored after ~17 h incubation.

Viability Plating. Viability was tested by a spot titer assay. For this, a 10-fold dilution series was prepared from overnight cultures, and 5  $\mu$ L of each dilution was spotted on to the appropriate plates, which were incubated at 37 °C overnight and imaged.

Metabolic Labeling of PG in Live Cells with TetraRh. For labeling live cells, most C. difficile strains were subcultured 1:100 into TY, grown to an OD<sub>600</sub> of 0.2 to 0.3, and metabolic label was added to a final concentration of 30  $\mu\text{M}$  . The LDT depletion strain was grown overnight in TY containing aTet at 4 ng/ $\mu$ L, washed once in TY to remove aTet, and then subcultured 1:100 into TY containing aTet at  $0.25 \text{ ng/}\mu\text{L}$ . TetraRh was added when the culture reached  $OD_{600} = 0.2$ . Typically about 1 mL of culture was incubated with dye. After 1 h at 37 °C, cells were washed three times with 1 mL phosphate-buffer saline (PBS), consisting of 137 mM NaCl, 3 mM KCl, 10 mM NaH<sub>2</sub>PO<sub>4</sub>, and 2 mM KH<sub>2</sub>PO<sub>4</sub>, pH 7.4). Washed cells were resuspended in 100  $\mu$ L PBS, and fixed by pipetting into 24  $\mu$ L fixation cocktail [4 μL 1 M NaPO<sub>4</sub> buffer, pH 7.4, and 20 μL 16% (wt/vol) paraformaldehyde (Alfa Aesar)]. Fixation was allowed to proceed at room temperature for 30 min, then on ice for 30 min. Fixed cells were washed three times in PBS, suspended in  $\sim$ 50  $\mu$ L PBS, then imaged by microscopy or analyzed by flow cytometry.

Microscopy. Cells were immobilized using thin agarose pads (1%). Phasecontrast micrographs were recorded on an Olympus BX60 microscope equipped with a 100× UPlanApo objective (numerical aperture, 1.35). Micrographs were captured with a Hamamatsu Orca Flash 4.0 V2+ complementary metal oxide semiconductor camera. Excitation light was generated with an X-Cite XYLIS light-emitting diode light source. Membranes were stained with the lipophilic dye FM4-64 (Life Technologies) at 10  $\mu$ g/mL. Cells were imaged immediately without washing. Red fluorescence was detected with the Chroma filter set 49008 (538 to 582 nm excitation filter, 587 nm dichroic mirror, and a 590 to 667 nm emission filter). Fluorescence was quantitated using the image analysis package Fiji (67). The plug-in module MicrobeJ was used to measure cell length (68).

Flow Cytometry. Fixed cells labeled with D-Ala-TetraRh or L-Ala-TetraRh were analyzed at the Flow Cytometry Facility at the University of Iowa using a Becton Dickinson LSR II instrument with a 561 nm laser, a 610/20-nm-band-pass filter, and a 600 LP dichroic filter as previously described (69). The data were analyzed using BD FACSDiva software. Fluorescence was quantitated at 900 V and the mean reported from 20,000 cells.

PG Purification and Muropeptide Analysis. For details of the following procedures, see SI Appendix. PG purification was purified from cells grown in 100 mL TY to an OD<sub>600</sub> of 0.3 following published procedures (70–72). PG purified from 100 mL of culture was digested with Mutanolysin (Sigma), reduced using NaBH<sub>4</sub> and separated using HPLC as previously described (73). Muropeptide peaks were collected and further purified individually on the HPLC. These purified muropeptide peaks were collected, lyophilized, and used for mass spectrometry analyses and for in vitro analyses of LDT activity. Liquid chromatography-mass spectrometry (LC-MS) was performed as described (74) by reversed-phase chromatography (Waters BEH C18) using acidified water/MeOH gradients with the column eluents evaluated by electrospray ionization mass spectrometry in the positive ion mode with a Shimadzu LCMS 9030 (QTof).

Western Blot. Rabbit polyclonal antiserum against Ldt1, Ldt2, and Ldt3 was raised against purified protein (ProSci). To analyze protein levels by western immunoblotting, 3 mL cultures grown to an  $\text{OD}_{600} \sim 0.85$  were pelleted, resuspended in 300 µL 2× Laemmli buffer, and sonicated (Branson Sonifier 450, microtip, output 3, two cycles of 15 pulses). After heating at 95 °C for 10 to 15 min, 20  $\mu$ L sample was electrophoresed on 10% sodium dodecyl sulfate-polyacrylamide gel

electrophoresis (TGX gel, BioRad), transferred to nitrocellulose, and developed using standard laboratory procedures. Primary antiserum for Ldt1 and Ldt3 was used at 1:10,000; primary antiserum for Ldt2 was used at 1:100,000. Secondary antibody (IRDye 680LT goat anti-rabbit antibody, LI-COR, Lincoln, NE) was used at 1:10,000, and blots were visualized with an Azure Biosystems Sapphire Biomolecular Imager.

**Sporulation.** Effects of  $\mathit{Idt}$  mutation on the ability to sporulate were measured as previously described (75).

Production, Purification, and Circular Dichroism Spectroscopy of LDT. Expression strains were grown in 1 LLB Amp <sup>100</sup> Cm<sup>10</sup> at 37 °C to an OD<sub>600</sub> of 0.5, induced with 1 mM IPTG, shifted to 30 °C, grown an additional 3 h, and harvested at 8,000 × q. Proteins were purified at 4 °C by the batch method over 1 mL Ni-NTA resin according to the manufacturer's instructions (HisPur, Thermo Scientific). All buffers were 50 mM NaPO<sub>4</sub>, pH 7.4, and 100 mM NaCl, with varied imidazole (10 mM lysis buffer, 20 mM wash buffer, and 250 mM elution buffer). The eluted protein was dialyzed against 50 mM NaPO<sub>4</sub>, pH 7.4, and 100 mM NaCl and either stored at 4 °C or adjusted to 5% glycerol and stored at -80 °C. Circular dichroism spectroscopy to determine protein secondary structure was performed with about  $5 \mu M$  protein in  $50 \text{ mM NaPO}_4$ , pH 7.0, 50 mM NaCl as described (76).

LDT Assay with TetraRH and Purified Sacculi. PG sacculi for in vitro labeling were purified from B. subtilis as outlined for C. difficile above, except that PG was incubated with 48% hydrofluoric acid (Sigma) instead of 6 N HCl to remove teichoic acids (71). Sacculi were adhered to poly-L-Lysine coated multiwell slides as previously described (77). Any free poly-L-lysine coated surface was blocked with 2 mg/mL bovine serum albumin for 20 min and washed with PBS. For the reaction,  $5 \mu M$  enzyme was premixed with  $30 \mu M$  fluorescent substrate analog in 50 mMNaPO<sub>4</sub>, pH 7.0, and 50 mM NaCl. The reaction was started by pipetting 10 μL to the well with the PG sacculi and incubated at 37 °C for 1 h. Wells were washed with PBS and imaged by microscopy. To measure inhibition by meropenem (AuroMedics Pharma LLC, ordered from the University of Iowa hospital pharmacy), the antibiotic was added to the enzyme-TetraRh mixture, incubated 5 min at room temperature, then pipetted onto the immobilized PG sacculi and processed as above. After imaging, average fluorescence intensity was quantitated for a minimum of 10 sacculi per condition using Fiji. IC50 values were determined by performing a nonlinear fit (inhibitor vs. response, three parameters) using GraphPad Prism v10.2.0, with the top value constrained to 100% and the bottom to 0.

LDT Assay with Purified DS-TetraP. LDTs were assayed much as described (24) in 50 mM NaPO<sub>4</sub>, pH 7.0, and 50 mM NaCl at 10 μM enzyme and 30 μM DS-TetraP substrate (purified from R20291) in a final volume of 12  $\mu$ L. As the purified substrate had been reduced prior to HPLC purification, the MurNAc was converted to the alcohol form. Assays were incubated at 37 °C for 2 h prior to chilling to 4 °C and HPLC analysis using the same acetonitrile/trifluoracetic acid buffer system and peak detection at 206 nm as described above for the muropeptide analysis.

Sequence Alignments. VanW domain sequences were aligned in Clustal Omega using default parameters as described in SI Appendix.

Domain Modeling. The VanW and YkuD domains were modeled with AF2 (36) using MMseqs2 (78) by running ColabFold v1.5.5 (79). The following parameters were used: msa\_mode: mmseq2\_uniref\_env, pair\_mode: unpaired\_pair, model\_type: auto, num\_recycles: 3, recycle\_early\_stop\_tolerance: auto, relax\_ max\_iterations: 200, pairing\_strategy: greedy. The highest-ranked structure by predicted local difference test was used for illustrations. AF2 structures were rendered in ChimeraX version 1.5 using default settings (80). Structure comparison (overlay) was performed using the matchmaker function in ChimeraX using the "best-aligning pair of chains between reference and match structure".

Phylogenetic Distribution of VanW Domains. The phylogenetic distribution of VanW domains was determined by searching PF04294 in AnnoTree version 2.0 beta (46), which includes Kyoto Encyclopedia of Genes and Genomes (KEGG) and InterPro annotations for 80,789 bacterial and 4,416 archaeal genomes.

Data, Materials, and Software Availability. The whole-genome sequencing data of the  $\Delta ldt1-3$  mutant were deposited under the BioProject ID PRJNA1125457 (81). RNA-seq data were submitted to the NCBI GEO repository and assigned accession number GSE270128 (82). All other data are included in the manuscript or SI Appendix.

ACKNOWLEDGMENTS. The following reagent was obtained through the ATCC: Paraclostridium bifermentans ATCC 638. The following reagents were obtained through Biodefense and Emerging Infections Resources, NIAID, NIH as part of the Human Microbiome Project: Eubacterium sp., Strain AS15, HM-766; Ruminococcaceae sp., Strain D16, HM-79; and Lachnospiraceae sp., Strain 5\_1\_57FAA, HM-157. This work was supported by the NIH (R01Al155492 to D.S.W. and C.D.E., R01GM138630 to D.L.P., and R35GM124893-06 to M.M.P.) The LC-MS work was funded by GlycoMIP, a NSF Materials Innovation Platform funded through Cooperative Agreement DMR-1933525. Cell fluorescence was quantitated at the Flow Cytometry Facility, a core research facility at the University of Iowa funded through user fees and the generous financial support of the Carver College of Medicine, Holden Comprehensive Cancer Center, and Iowa City

Veteran's Administration Medical Center. RNA integrity was characterized by the Genomics Division of the Iowa Institute of Human Genetics, which is supported, in part, by the University of Iowa Carver College of Medicine. We thank Johann Peltier for sharing information prior to publication, Atsushi Yahashiri for sharing B. subtilis PG sacculi and members of the Ellermeier and Weiss laboratories for helpful discussions.

Author affiliations: <sup>a</sup>Department of Microbiology and Immunology, Carver College of Medicine, University of Iowa, Iowa City, IA 52242; <sup>b</sup>Department of Chemistry, University of Virginia, Charlottesville, VA 22904; <sup>c</sup>Department of Biochemistry, Virginia Tech, Blacksburg, VA 24061; <sup>d</sup>Department of Biological Sciences, Virginia Tech, Blacksburg, VA 24061; and <sup>e</sup>Graduate Program in Genetics, University of Iowa, Iowa City, IA 52242

- Centers for Disease Control and Prevention, "Antibiotic resistance threats in the United States" (US Department of Health and Human Services, Centers for Disease Control and Prevention, Atlanta, GA, 2019). http://dx.doi.org/10.15620/cdc:82532. Accessed 2 December 2023.
- T. D. Lawley et al., Targeted restoration of the intestinal microbiota with a simple, defined bacteriotherapy resolves relapsing Clostridium difficile disease in mice. PLoS Pathog. 8, e1002995
- $S.\ Khanna\ \textit{et al.}, The\ epidemiology\ of\ community-acquired\ \textit{Clostridium\ difficile}\ in fection:\ A$ population-based study. Am. J. Gastroenterol. 107, 89-95 (2012).
- D. A. Leffler, J. T. Lamont, Clostridium difficile Infection. N. Engl. J. Med. 373, 287-288 (2015).
- S. A. Cole, T. J. Stahl, Persistent and recurrent Clostridium difficile colitis. Clin. Colon Rectal. Surg. 28, 65-69 (2015).
- T. J. Louie et al., Fidaxomicin versus vancomycin for Clostridium difficile infection. N. Engl. J. Med. 364, 422-431 (2011).
- P. D. A. Rohs, T. G. Bernhardt, Growth and division of the peptidoglycan matrix. Annu. Rev. Microbiol. 75, 315-336 (2021).
- W. Vollmer, D. Blanot, M. A. de Pedro, Peptidoglycan structure and architecture. FEMS Microbiol. Rev. 32, 149-167 (2008).
- B. Glauner, J. V. Höltje, U. Schwarz, The composition of the murein of Escherichia coli. J. Biol. Chem. 263, 10088-10095 (1988).
- S. Magnet, L. Dubost, A. Marie, M. Arthur, L. Gutmann, Identification of the L,D-transpeptidases for peptidoglycan cross-linking in Escherichia coli. J. Bacteriol. 190, 4782-4785 (2008).
- J. C. Quintela, M. Caparros, M. A. de Pedro, Variability of peptidoglycan structural parameters in gram-negative bacteria. FEMS Microbiol. Lett. 125, 95-100 (1995).
- A. Aliashkevich, F. Cava, L,D-transpeptidases: The great unknown among the peptidoglycan crosslinkers. FEBS J. 289, 4718–4730 (2022).
- G. Stankeviciute et al., Differential modes of crosslinking establish spatially distinct regions of
- peptidoglycan in Caulobacter crescentus. Mol. Microbiol. 111, 995-1008 (2019). K. Costa et al., The morphological transition of Helicobacter pylori cells from spiral to coccoid is
- preceded by a substantial modification of the cell wall. J. Bacteriol. 181, 3710-3715 (1999). M. A. Snowden, H. R. Perkins, Peptidoglycan cross-linking in Staphylococcus aureus. An apparent
- random polymerisation process. Eur. J. Biochem. 191, 373-377 (1990). J. A. F. Sutton et al., Staphylococcus aureus cell wall structure and dynamics during host-pathogen
- interaction. PLoS Pathog. 17, e1009468 (2021). C. Baranowski et al., Maturing Mycobacterium smegmatis peptidoglycan requires non-canonical
- crosslinks to maintain shape. Elife 7, e37516 (2018). 18. P. J. Brown et al., Polar growth in the Alphaproteobacterial order Rhizobiales. Proc. Natl. Acad. Sci.
- U.S.A. 109, 1697-1701 (2012).
- E. Sauvage, F. Kerff, M. Terrak, J. A. Ayala, P. Charlier, The penicillin-binding proteins: Structure and role in peptidoglycan biosynthesis. *FEMS Microbiol. Rev.* **32**, 234–258 (2008). J. L. Mainardi *et al.*, A novel peptidoglycan cross-linking enzyme for a beta-lactam-resistant transpeptidation pathway. *J. Biol. Chem.* **280**, 38146–38152 (2005). 20.
- J. L. Mainardi et al., Unexpected inhibition of peptidoglycan LD-transpeptidase from Enterococcus
- faecium by the beta-lactam imipenem. J. Biol. Chem. 282, 30414-30422 (2007)
- J. Peltier et al., Clostridium difficile has an original peptidoglycan structure with a high level of N-acetylglucosamine deacetylation and mainly 3-3 cross-links. J. Biol. Chem. 286, 29053-29062
- M. Dembek et al., High-throughput analysis of gene essentiality and sporulation in Clostridium difficile. mBio 6, e02383 (2015).
- L. Sütterlin, Z. Edoo, J. E. Hugonnet, J. L. Mainardi, M. Arthur, Peptidoglycan cross-linking activity of I, d-transpeptidases from Clostridium difficile and inactivation of these enzymes by beta-lactams. Antimicrob. Agents Chemother. 62, e01607-17 (2018).
- 25. N. F. Galley et al., Clostridioides difficile canonical L, D-transpeptidases catalyze a novel type of peptidoglycan cross-links and are not required for beta-lactam resistance. J. Biol. Chem. 300, 105529 (2024).
- J. J. Lu, C. L. Perng, M. F. Ho, T. S. Chiueh, W. H. Lee, High prevalence of VanB2 vancomycin-resistant Enterococcus faecium in Taiwan. J. Clin. Microbiol. 39, 2140-2145 (2001).
- S. J. McKessar, A. M. Berry, J. M. Bell, J. D. Turnidge, J. C. Paton, Genetic characterization of vanG, a novel vancomycin resistance locus of Enterococcus faecalis. Antimicrob. Agents Chemother. 44 3224-3228 (2000)
- J. Bielnicki et al., B. subtilis ykuD protein at 2.0 A resolution: Insights into the structure and function of a novel, ubiquitous family of bacterial enzymes. Proteins 62, 144-151 (2006).
- P. D. Karp et al., The BioCyc collection of microbial genomes and metabolic pathways. Brief Bioinform. 20, 1085-1093 (2019).
- E. Cuenot et al., The Ser/Thr kinase PrkC participates in cell wall homeostasis and antimicrobial resistance in Clostridium difficile. Infect. Immun. 87, e00005-19 (2019).
- J. Mistry et al., Pfam: The protein families database in 2021. Nucleic Acids Res. 49, D412-D419 (2021).
- D. G. Conrady, J. J. Wilson, A. B. Herr, Structural basis for Zn2+-dependent intercellular adhesion in staphylococcal biofilms. Proc. Natl. Acad. Sci. U.S.A. 110, E202-E211 (2013).

- 33. N. Paukovich et al., Streptococcus pneumoniae G5 domains bind different ligands. Protein Sci. 28, 1797-1805 (2019).
- A. Ruggiero et al., Crystal structure of the resuscitation-promoting factor (DeltaDUF)RpfB from M tuberculosis. J. Mol. Biol. 385, 153-162 (2009).
- Y. R. Brunet, C. Habib, A. P. Brogan, L. Artzi, D. Z. Rudner, Intrinsically disordered protein regions are required for cell wall homeostasis in Bacillus subtilis. Genes. Dev. 36, 970-984 (2022).
- $J.\ Jumper\ \emph{et al.}, Highly\ accurate\ protein\ structure\ prediction\ with\ Alpha Fold.\ \emph{Nature}\ \textbf{596}, 583-589\ (2021).$
- S. Biarrotte-Sorin *et al.*, Crystal structure of a novel beta-lactam-insensitive peptidoglycan transpeptidase. J. Mol. Biol. 359, 533-538 (2006).
- N. A. Caveney et al., Structural insight into YcbB-mediated beta-lactam resistance in Escherichia coli. 38. Nat. Commun. 10, 1849 (2019).
- M. van Kempen et al., Fast and accurate protein structure search with Foldseek. Nat. Biotechnol. 42, 243-246 (2023).
- L. Holm, Using dali for protein structure comparison. Methods Mol. Biol. 2112, 29-42 (2020).
- L. Holm, A. Laiho, P. Toronen, M. Salgado, DALI shines a light on remote homologs: One hundred discoveries. Protein Sci. 32, e4519 (2023).
- A. J. Apostolos, N. J. Ferraro, B. E. Dalesandro, M. M. Pires, SaccuFlow: A high-throughput analysis platform to investigate bacterial cell wall interactions. ACS Infect. Dis. 7, 2483-2491 (2021).
- S. E. Pidgeon et al., L, D-transpeptidase specific probe reveals spatial activity of peptidoglycan cross-linking. ACS Chem. Biol. 14, 2185-2196 (2019).
- U. Müh, A. G. Pannullo, D. S. Weiss, C. D. Ellermeier, A xylose-inducible expression system and a CRISPR interference plasmid for targeted knockdown of gene expression in Clostridioides difficile. J. Bacteriol. **201**, e00711-18 (2019).
- S. El-Gebali et al., The Pfam protein families database in 2019. Nucleic Acids Res. 47, D427-D432 (2019)
- K. Mendler et al., AnnoTree: Visualization and exploration of a functionally annotated microbial tree of life. Nucleic Acids Res. 47, 4442-4448 (2019).
- M. Steinegger et al., HH-suite3 for fast remote homology detection and deep protein annotation. BMC Bioinform. 20, 473 (2019).
- S. B. Erdemli et al., Targeting the cell wall of Mycobacterium tuberculosis: Structure and mechanism of L, D-transpeptidase 2. Structure 20, 2103-2115 (2012).
- P. J. Stogios, A. Savchenko, Molecular mechanisms of vancomycin resistance. Protein Sci. 29,
- P. Courvalin, Vancomycin resistance in gram-positive cocci. Clin. Infect. Dis. 42, S25-S34 (2006).
- J. Cremniter et al., Novel mechanism of resistance to glycopeptide antibiotics in Enterococcus faecium. J. Biol. Chem. 281, 32254-32262 (2006).
- W. J. Shen et al., Constitutive expression of the cryptic  $vanG_{cd}$  operon promotes vancomycin resistance in Clostridioides difficile clinical isolates. J. Antimicrob. Chemother. **75**, 859–867 (2020).
- M. D. Sacco et al., A unique class of Zn(2+)-binding serine-based PBPs underlies cephalosporin resistance and sporogenesis in *Clostridioides difficile*. *Nat. Commun.* **13**, 4370 (2022).
- S. Shrestha, N. Taib, S. Gribaldo, A. Shen, Diversification of division mechanisms in endosporeforming bacteria revealed by analyses of peptidoglycan synthesis in Clostridioides difficile. Nat. Commun. 14, 7975 (2023).
- R. Gupta et al., The Mycobacterium tuberculosis protein LdtMt2 is a nonclassical transpeptidase required for virulence and resistance to amoxicillin. Nat. Med. 16, 466-469 (2010).
- J. É. Hugonnet, L. W. Tremblay, H. I. Boshoff, C. E. Barry III, J. S. Blanchard, Meropenem-clavulanate is effective against extensively drug-resistant Mycobacterium tuberculosis. Science 323, 1215-1218
- P. Kumar et al., Non-classical transpeptidases yield insight into new antibacterials. Nat. Chem. Biol.
- E. M. Steiner, G. Schneider, R. Schnell, Binding and processing of beta-lactam antibiotics by the transpeptidase Ldt(Mt2) from Mycobacterium tuberculosis. FEBS J. 284, 725-741 (2017).
- R. A. Stabler et al., Comparative genome and phenotypic analysis of Clostridium difficile 027 strains provides insight into the evolution of a hypervirulent bacterium. Genome Biol. 10, R102 (2009).
- S. S. Dineen, A. C. Villapakkam, J. T. Nordman, A. L. Sonenshein, Repression of *Clostridium difficile* toxin gene expression by CodY. *Mol. Microbiol.* **66**, 206–219 (2007).
- P. Trieu-Cuot, C. Carlier, C. Poyart-Salmeron, P. Courvalin, Shuttle vectors containing a multiple cloning site and a lacZ alpha gene for conjugal transfer of DNA from Escherichia coli to grampositive bacteria. Gene 102, 99-104 (1991).
- U. Müh, C. D. Ellermeier, D. S. Weiss, The WalRK two-component system is essential for proper cell envelope biogenesis in Clostridioides difficile. J. Bacteriol. 204, e0012122 (2022).
- K. N. McAllister, L. Bouillaut, J. N. Kahn, W. T. Self, J. A. Sorg, Using CRISPR-Cas9-mediated genome editing to generate C. difficile mutants defective in selenoproteins synthesis. Sci. Rep. 7, 14672
- G. M. Kaus et al., Lysozyme resistance in Clostridioides difficile is dependent on two peptidoglycan deacetylases. J. Bacteriol. 202, e00421-20 (2020).
- B. R. Zbylicki et al., Identification of Clostridioides difficile mutants with increased daptomycin resistance. J. Bacteriol. 206, e0036823 (2024).

- A. G. Pannullo, Z. Guan, H. Goldfine, C. D. Ellermeier, HexSDF is required for synthesis of a novel glycolipid that mediates daptomycin and bacitracin resistance in C. difficile. mBio 14, e0339722 (2023).
- J. Schindelin et al., Fiji: An open-source platform for biological-image analysis. Nat. Methods 9, 676–682 (2012).
- A. Ducret, E. M. Quardokus, Y. V. Brun, MicrobeJ, a tool for high throughput bacterial cell detection and quantitative analysis. *Nat. Microbiol.* 1, 16077 (2016).
- E. M. Ransom, G. M. Kaus, P. M. Tran, C. D. Ellermeier, D. S. Weiss, Multiple factors contribute to bimodal toxin gene expression in *Clostridioides (Clostridium) difficile*. Mol. Microbiol. 110, 533–549 (2018).
- T. D. Ho et al., Clostridium difficile extracytoplasmic function sigma factor sigmaV regulates lysozyme resistance and is necessary for pathogenesis in the hamster model of infection. Infect. Immun. 82, 2345–2355 (2014).
- D. C. McPherson, D. L. Popham, Peptidoglycan synthesis in the absence of class A penicillin-binding proteins in *Bacillus subtilis. J. Bacteriol.* 185, 1423–1431 (2003).
- K. Hayashi, A rapid determination of sodium dodecyl sulfate with methylene blue. Anal. Biochem. 67, 503-506 (1975).
- D. L. Popham, J. Helin, C. E. Costello, P. Setlow, Analysis of the peptidoglycan structure of *Bacillus subtilis* endospores. *J. Bacteriol.* 178, 6451–6458 (1996).
- T. G. DeHart, M. R. Kushelman, S. B. Hildreth, R. F. Helm, B. L. Jutras, The unusual cell wall of the Lyme disease spirochaete *Borrelia burgdorferi* is shaped by a tick sugar. *Nat. Microbiol.* 6, 1583–1592 (2021).

- A. N. Edwards, S. M. McBride, Determination of the in vitro sporulation frequency of Clostridium difficile. Bio. Protoc. 7, e2125 (2017).
- L.T. Lewerke, P. J. Kies, U. Muh, C. D. Ellermeier, Bacterial sensing: A putative amphipathic helix in RsiV is the switch for activating sigmaV in response to lysozyme. PLoS Genet. 14, e1007527 (2018).
- A. Yahashiri, M. A. Jorgenson, D. S. Weiss, Bacterial SPOR domains are recruited to septal peptidoglycan by binding to glycan strands that lack stem peptides. *Proc. Natl. Acad. Sci. U.S.A.* 112, 11347–11352 (2015).
- M. Steinegger, J. Soding, MMseqs2 enables sensitive protein sequence searching for the analysis of massive data sets. Nat. Biotechnol. 35, 1026–1028 (2017).
- M. Mirdita et al., ColabFold: Making protein folding accessible to all. Nat. Methods 19, 679–682 (2022).
- E. F. Pettersen et al., UCSF ChimeraX: Structure visualization for researchers, educators, and developers. Protein Sci. 30, 70-82 (2021).
- K. W. Bollinger, D. S. Weiss, C. D. Ellermeier, C. difficile ldt mutant chromosome sequencing. NCBI BioProject. https://www.ncbi.nlm.nih.gov/bioproject/?term=PRJNA1125457 (2024). Deposited 18 June 18 2024.
- K. W. Bollinger, D. S. Weiss, C. D. Ellermeier, Identification of a new family of peptidoglycan transpeptidases reveals unusual crosslinking is essential for viability in C. difficile. NCBI GEO. https://www.ncbi.nlm.nih.gov/geo/query/acc.cgi?acc=GSE270128. Deposited 18 June 2024.